

NP Internal Report 72-15  
7 July 1972

MULTILAYER RELATIVISTIC RISE DETECTOR PROPOSAL  
FOR THE 300 GeV

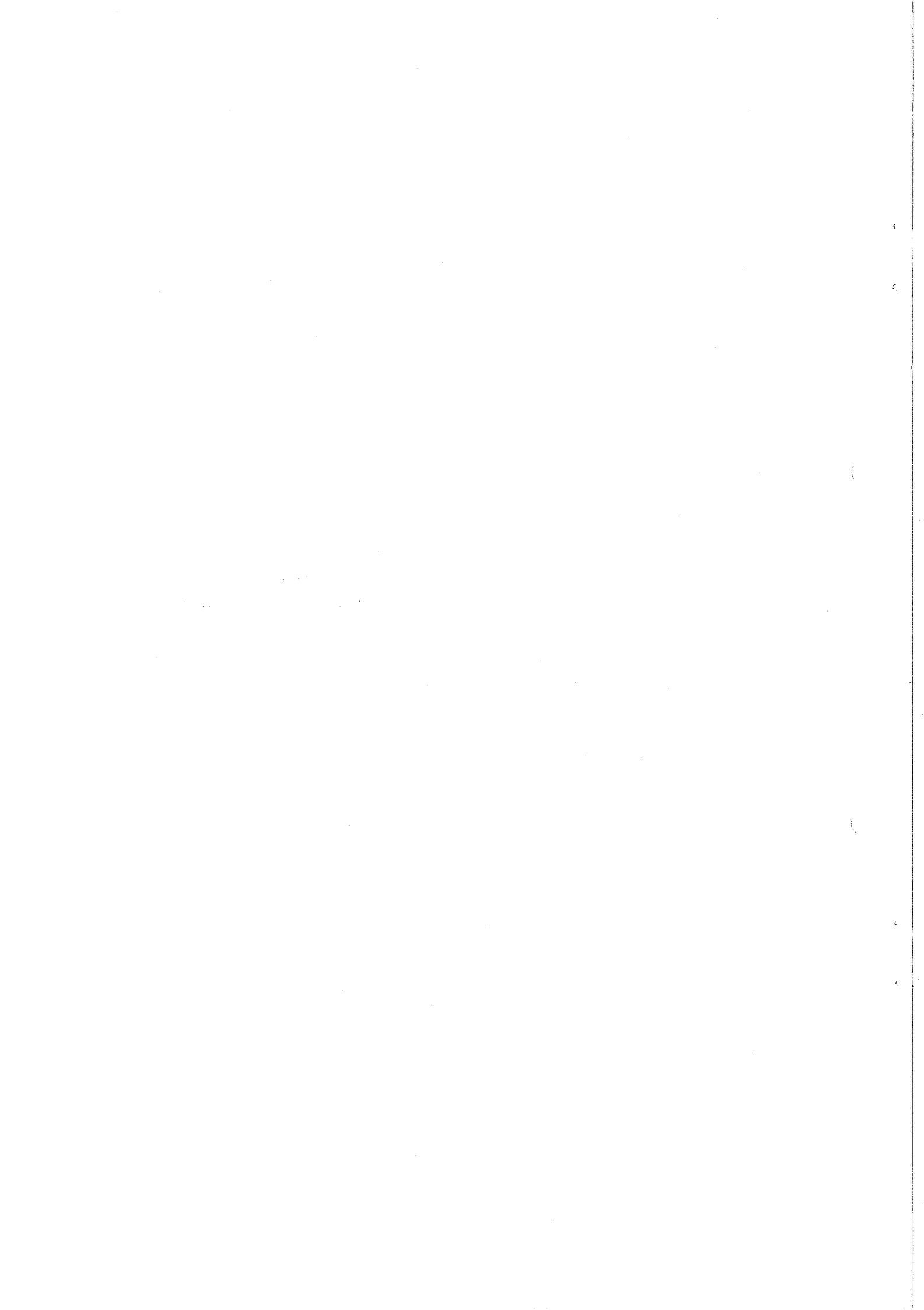
Z. Dimčovski

ABSTRACT

A new kind of detector is proposed for the 300 GeV accelerator particles after a review of recent work done at CERN on ionization counters. The detector consists of 200 to 400 (if the momentum region up to 300 GeV/c is to be explored) multiwire proportional chamber layers (3 mm wire spacing, 1 cm thick). Experimental tests of a 30-layer detector have shown promising features. Curves are presented giving the separation of various particles for the 300 GeV machine.

G E N E V A

1972



## 1. BASIC FACTS ABOUT ENERGY LOSS SPECTRA

When a monoenergetic beam of charged particles traverses a thin absorber the resulting energy-spectrum is not Gaussian but has a characteristic "Landau" <sup>1)</sup> tail on the side of the high-energy losses. The peak value of  $dE/dx$  is called the most probable energy loss  $\Delta_0$ , which is systematically smaller than the mean energy loss  $\bar{\Delta}$ . The bigger the ratio  $\bar{\Delta}/\Delta_0$ , which is inversely proportional to the thickness of the medium, the bigger the asymmetry is [for thick absorbers the distribution is approximately Gaussian]. If  $\Delta_0$  is plotted versus the Lorentz factor  $\gamma$ , a universal curve is obtained, as shown in Fig. 1. The increase of  $\Delta_0$  as a function of  $\gamma$  is not linear for  $\gamma > 100$ ; this is due to the so-called density effect (polarization of the neighbouring atoms which produce a field in an opposite direction to the radiated field). This saturation region, reached for  $\gamma \gtrsim 1000$ , is referred to as the Fermi plateau.

Landau has given the theoretical shape of the ionization loss distribution using some approximations (atomic electrons considered as free, and no upper limit in the energy transfer). More recent theories have tried to improve the treatment; Vavilov<sup>2)</sup> has introduced a cut-off in the energy transfer, and Blunck et al.<sup>3)</sup> have taken into account the electron binding energies and the bremsstrahlung losses, using some other approximations.

Figure 2 gives the Landau spectra for 100 GeV  $\pi$  and p for 1 cm of A (NTP) traversed. It is the considerable overlap between the two spectra that limits the use of this effect for particle separation (we will see in Section 2.2 how it is possible to overcome this drawback).

Solids and liquids are less favourable than gases for particle separation because: a) due to the density effect, the ratio of  $dE/dx$  at the Fermi plateau to  $dE/dx$  at minimum ionization is smaller than for gases; b) better statistics (and efficiency) can be obtained with gases where a loss of about 26 eV is necessary to produce an ion pair (for A), while in the case of solid scintillators, on the average only one photoelectron is produced on the photocathode for 1 keV loss; c) for a given thickness there is a smaller multiple scattering for gases (factor of  $10^3$  in density).

## 2. SOME RECENT DEVELOPMENTS ON IONIZATION DETECTORS AT CERN

### 2.1 Introduction

Although the first gas proportional counters were built already in 1908 (Rutherford and Geiger), it is only recently that they have been used in large scale operation, due to conceptual and technical reasons. A fundamental advance concerning the concept is due to Charpak et al. with the multiwire proportional chamber (MWPC)<sup>4)</sup> which in fact introduced the proportional counter in the quite restrictive family of high-energy detectors. The technical reasons are mainly the advances in electronics and data processing which are well known.

The MWPC is convenient both for: localization (or track reconstruction) and particle identification (simple  $dE/dx$  method). These two functions can be achieved in the same detector, using for the first the information on the sensitive wires and for the second the electrodynamic image of the sensitive wire pulses on the high-voltage electrode (see Fig. 3).

Different gases such as A, CO<sub>2</sub>, isobutane, He, C<sub>3</sub>H<sub>8</sub>, etc., have been used showing different properties<sup>5)</sup>. One of them, the so-called "magic mixture", has allowed a very simple electronics per wire (with a gas amplification gain  $\sim 100$  times that of the gases normally used) in the case when only the trajectory reconstruction is required, which can be very useful when the two functions are separated. The chambers actually built have a size ranging from  $\leq 100$  cm<sup>2</sup> to several m<sup>2</sup>, and wire spacing going down to 1 mm [ $\sigma(\text{localization}) = 0.35$  mm per chamber]. Under a voltage of a few kV a plateau of 100% efficiency over a few hundred volts is currently reached. For more details as well as for a few aspects not mentioned here (e.g. time jitter, electronegative gases, amplification factor, etc.), see other papers<sup>5,6)</sup>.

At the present time there are already many groups at CERN and elsewhere using MWPC, mainly for "yes-no" information. The situation concerning the proportional information is considerably poorer; this is briefly reviewed in the next section.

## 2.2 Use of the dE/dx information for particle identification

It was remarked in Section 1 (see Fig. 2) that owing to a considerable overlap, one dE/dx measurement is not sufficient to separate two kinds of particles, even if they have a big dE/dx difference. In such conditions only a statistical method (a series of N measurements, N being the number of detectors, simultaneous and independent for one given particle) can overcome this difficulty. This is an old idea [from Landau's<sup>1)</sup> original paper in 1944!] which could be realized only recently for reasons mentioned in Section 2.1. Recently, various attempts have been made to apply this method to a particular problem.

The practical application of the method was initiated by Alikhanov et al.<sup>7)</sup>, who used five counters for a cosmic-ray study. Ramana-Murthy et al.<sup>8)</sup> extrapolated, by means of Monte Carlo simulation, the data from one counter to a 6 to 12 counter cascade for cosmic  $\pi$  and p of 100 GeV (and  $\mu$  and K).

A detector recently built at CERN<sup>9)</sup> has used 30 MWPC (the largest number of proportional layers ever built for energy loss sampling purposes). Each layer has  $10 \times 10$  cm<sup>2</sup> size and is 1 cm thick (in the beam direction). The detector was intended to study the  $\pi^-/e$  separation in a beam of variable momentum from the CERN 600 MeV Synchro-cyclotron; in this way the whole region between the minimum ionization and the Fermi plateau was explored. Because of the big values of  $\gamma$  for the electrons (up to  $\sim 10^3$ ), this study is a simulation of the highest energy particles produced in proton accelerators available now or in the near future. In spite of non-optimized instrumental conditions (gas amplification gain varying by 10% from wire to wire and linearity in the associated electronics  $\sim 5\%$ ) an effective separation between  $\pi^-$  and e was achieved. The method was found to be successful for separation of two populations ( $\pi^-$  and e) differing by a factor  $\sim 10^2$  in magnitude (the contamination of typically 1% e in a  $\pi^-$  beam was observed experimentally). Discrepancies with the theories mentioned in Section 1 were found. The most striking one is the lowest value for the height of the Fermi plateau. When compared to the value at minimum ionization a typical increase of 45% was observed, although Sternheimer's theory predicts 78% even without taking into account the

radiative correction for  $e$ . On the other hand, Landau's theory underestimates the width of the ionization curves, although Blunck's overestimates it (even without taking into account the finite energy resolution of the MWPC  $\sim 20\%$ ) (Fig. 4). The discrepancies mentioned above are found also by other authors<sup>10,11</sup>). An interesting observation is the non-correlation between the layers. If there were any correlation between the  $\delta$ -rays emitted in one chamber and traversing the neighbouring ones, this method of sampling could have run into difficulties. This was checked experimentally by imposing an energy loss in a variable "window" in one chamber and looking for correlation in the forward and backward neighbours. No observable effect was found, which is what is expected because of the small value of the energy losses (typically  $\sim$  a few keV), and the small range of the  $\delta$ -rays at these energies.

Recently C. Rubbia has written a proposal for a multilayer relativistic detector for the ISR<sup>12</sup>). The experimental results with one proportional counter were used and extended by Monte Carlo simulation to a 50 layer counter. At the present time, Rubbia et al. are preparing a system of 30 proportional counters system for a quark search at the ISR<sup>13</sup>). The system has obvious advantages when compared to an equivalent scintillator device (see Section 1).

I. Lehraus, D. Jeanne and R. Matthewson have built and successfully tested single wire proportional detectors using the relativistic rise<sup>14</sup>). Lehraus<sup>15</sup>) has recently sent a proposal to the ECFA Working Party on BEBC hybridization on a multilayer one-wire-proportional system to be used in conjunction with BEBC in the 50-200 GeV/c region. This system can perform the identification of the various particles which have the trajectories recorded by BEBC.

The work done by Calligaris et al.<sup>16</sup>) should be mentioned also, although only the lower region of the minimum ionizing loss curve was explored. It has been shown that six gas proportional counters can perform a p, d, t separation in low energies ( $\sim 10$  MeV) and therefore the flexibility of the energy loss sampling method is proved.

The few topics mentioned in this section show the rising interest in this method of energy loss sampling as a powerful tool in very high energy particle separation.

### 3. CONCEPT OF THE MULTILAYER RELATIVISTIC RISE DETECTOR FOR THE 300 GeV

#### 3.1 Physics of the detector

It is natural to extend the application of the multilayer proportional detector for the separation of the 300 GeV machine particles. Figure 5 gives Sternheimer's<sup>17)</sup> estimate for the average energy loss of  $\mu$ ,  $\pi$ , K, and p between 0.1 and 500 GeV/c<sup>18)</sup>.

One can see that above the intersecting region (2-3 GeV/c, where classical detectors are sufficient) the separation is adequate up to the upper limit in momentum, apart from the  $\mu$  and  $\pi$  for  $\vec{p} \gtrsim 100$  GeV/c. If muons are detected by an absorption detector there are mainly pions, kaons and protons left unidentified, whose most pessimistic difference in ionization is  $\sim 5\%$  at 300 GeV/c.

In order to estimate how many layers are necessary for a given rejection rate, a Monte Carlo simulation using recent experimental results<sup>9)</sup> was performed as described below. Given two kinds of particles A and B, the following empirical function is used to represent the energy loss spectra:

$$y(x) = \begin{cases} = \exp\left(-\frac{x^2}{40}\right) & \text{for } x \leq 0 \\ 1.65 \times \exp\{-0.5 [0.2x + \exp(-0.15x)]\} & \text{for } x \geq 0 \end{cases}$$

for particles A, where  $x = dE/dx - \Delta_0$  (i.e. the origin of x is taken arbitrarily at  $\Delta_0$ ). The same analytic expression shifted on the x axis by a given amount sh ( $sh = \Delta_{0B} - \Delta_{0A} \geq 0$ ), was used to simulate the population B (the two curves have the same width). The fit is compared to experimental data and Landau's and Blunck's theories in Fig. 4.

Apart from the fact that the curves are of simple analytic form (which is not the case for the two theoretical distributions), such a simulation has obvious advantages over one done on a formal basis only. It is more realistic also, because then the intrinsic energy resolution of the counter (varying like  $1/\sqrt{dE/dx}$ ) and the jitter of the electronics are taken into account (which together give an additional flattening of the curves of  $\sim 20\%$ ).

Under such conditions various data reduction methods are applied in order to fix the number  $N$  of layers that are necessary in order to have a given overlap between the two spectra. They are:

- a) the distribution of the average of the  $N$  pulses [with the variant<sup>19)</sup>: distribution of the average of the subset of  $N_S$  ( $N_S < N$ ) smallest pulses];
- b) the distribution of the average logarithms of  $N$  pulses [with the variant analogous to (a)];
- c) the maximum likelihood ratio where for a given event (and  $N$  measurements of  $dE/dx = x_i$ ) the ratio

$$M_L = \frac{\prod_{i=1}^N y(x_i)_A}{\prod_{i=1}^N w(x_i)_B}$$

is evaluated, where the  $x_i$ ,  $y$ , and  $w$  are the energy losses, the spectrum for particles A, and the spectrum for particles B, respectively [ $y(x_i) = w(x_i + sh)$ ].

The method (c) is found to give the best separation<sup>8,9)</sup>.

Figures 6, 7 and 8 show which separation can be expected with 200, 400 or 600 layers for the most pessimistic energy loss difference (5% at 300 GeV/c). For lower momenta this difference can go up to 17%.

Figures 9 and 10 show the separation obtained with 200 and 400 layers for a 10% increase in  $\Delta E/\Delta x$ ; Figs. 11 and 12 show a separation with 200 and 400 layers for 15%.

This estimate is somewhat pessimistic because an equal width was assumed for the two distributions of particles, which is not true experimentally<sup>8,9,11,20)</sup>. Recent experimental data<sup>9)</sup> have shown that going from the minimum ionizing particles up to the Fermi plateau a broadening of  $\sim 35\%$  of the ionization loss curve can be expected. Figure 13 is for the same conditions as those of Fig. 10, but the width in the  $dE/dx$  curve for particles B was assumed to be 20% larger than for A. An unexpected effect, probably due to the quenching agents in the gas mixtures, was recently discovered<sup>9)</sup>; it results in a quenching of the relativistic increase and a flattening of the B curve by 100%! It was found that if



a special gas (argon + isobutane) is used, a separation can be achieved for particles having the same most probable energy loss! (The separation is explained by the fact that the likelihood method is sensitive to the shape of these curves.)

The simulation done previously is valid for experimental layers of  $\sim 1$  cm gas thickness. If thicker layers ( $\sim 50$  cm) are used, the separation is better (because the curves have a "Gaussian-like" shape) but is prohibitive for the total size of the multilayer detector. A thickness of  $\sim 1$  cm (up to 5) and a wire spacing of  $\sim 3$  mm seem most appropriate for this proposal for ease of construction and operation.

The number of layers given above can be decreased also if a worse rejection can be accepted or a limit of  $< 300$  GeV/c is studied. Concerning the rejection, one should notice that it results only in a loss in statistics and not in any kinematic bias (because of the nature of the Landau distribution). For this reason even a considerably bigger rejection is acceptable, which still can give a confidence level close to 100% for the unrejected events.

The proposed detector seems appropriate also for heavy mass and quark searches where large differences in ionization are expected.

### 3.2 Practical set-up. Alternatives for the electronics

If in an experimental set-up, one hodoscope placed before and one after the multilayer counter perform the trajectory reconstruction, its construction is particularly simple. Here we will consider the more ambitious system where particle identification and, simultaneously, trajectory reconstruction are obtained from one detector (a simplified scheme of the set-up is given in Fig. 14).

There are at least two alternative ways of doing this (see Fig. 3):

- a) only the sensitive wires will give the information: in terms of electronics the signal is split in two, one part giving the position after digitization, the other part giving the  $dE/dx$  after mixing of all the sensitive wires (ADC);
- b) the high-voltage plane is also used (see p. 2 and Fig. 3); the functions are separated.

The two solutions (a) and (b) are based on the same physical method and should give the same result.

A technical comparison between (a) and (b) as well as a cost comparison with other detectors will be given later in another note.

The question whether the reconstruction function has to be performed in every layer will also be discussed later (this will give a precision of  $1.5/\sqrt{N}$  mm, which may be redundant).

#### 4. CONCLUSIONS

The detector can operate in the region 5-300 GeV, and separates particles even when they are not constrained to be parallel (i.e. as in the DISC Čerenkov counter). It should be pointed out that apart from the detection of electrons, the transition radiation detector is useful above this region. When the multilayer relativistic rise detector is used in conjunction with a transition radiation detector<sup>21)</sup>, one has a powerful detector for the full range from a few to the thousands GeV region.

The main advantages of the multilayer relativistic rise detector can be listed as follows:

- a) it is a unique detector for this energy region, which can perform both the identification and trajectory reconstruction simultaneously;
- b) it is sensitive simultaneously to all kinds of particles in the whole  $p$  region;
- c) it accepts multiparticle events;
- d) there are no problems with divergent beams;
- e) its cost is low in comparison with equivalent detectors.

I am indebted to G. Charpak who aroused my interest in this subject. Many stimulating discussions with J.V. Allaby, U. Amaldi, W. Bartel, R. Biancastelli, C. Bosio, G. Cocconi, A.N. Diddens, R.W. Dobinson, J. Litt, G. Matthiae and A.M. Wetherell are gratefully acknowledged. Thanks are due to K. Kuroda, A. Minten, E. Picasso, C. Rubbia, J. Steinberger, M. Vivargent and L.C. Yuan for critical reading of the manuscript.

REFERENCES

- 1) L. Landau, J. Phys. Vol. V1, No. 4, 201 (1944).
- 2) P.V. Vavilov, JETP 5, No. 4, 749 (1957).
- 3) O. Blunck and K. Westphal, Z. Phys. 130, 641 (1951).
- 4) G. Charpak, R. Bouclier, T. Bressani, J. Favier and Č. Zupančič, Nuclear Instrum. Methods 62, 235 (1968).
- 5) R. Bouclier, G. Charpak, Z. Dimčovski, G. Fisher, F. Sauli, G. Coignet and G. Flügge, Nuclear Instrum. Methods 88, 149 (1970).
- 6) Z. Dimčovski, CERN NP internal report 70-16 (1970).
- 7) A. Alikhanov, V. Lubimov and G. Elisejev, Proc. Conf. on High-Energy Physics, CERN (1956), p. 87.
- 8) P. Ramana-Murthy and G. Demester, Nuclear Instrum. Methods 56, 93 (1967).
- 9) Z. Dimčovski, J. Favier, G. Charpak and G. Amato, Nuclear Instrum. Methods 151, 94 (1971).  
Z. Dimčovski, thesis, University of Grenoble, October 1970 and CERN NP internal report 70-30 (1970).
- 10) D. West, Proc. Phys. Soc. A 66, 306 (1953).
- 11) P.V. Ramana-Murthy, Nuclear Instrum. Methods 63, 77 (1968).
- 12) C. Rubbia, CERN NP internal report 70-25 (1970).
- 13) C. Rubbia's group (private communication).
- 14) I. Lehraus and D. Jeanne, Nuclear Instrum. Methods 93, 257 (1971).  
I. Lehraus and R. Matthewson, Nuclear Instrum. Methods 97, 187 (1971).
- 15) I. Lehraus, Paper submitted to ECFA working group on BEBC hybridization (March 1972).
- 16) F. Calligaris, C. Cernigoi and K. Ziock, CERN-PH III 70/2 (proposed to Physics III Committee).
- 17) R.M. Sternheimer, Phys. Rev. 115, 137 (1959); 88, 851 (1952); 103, 511 (1956).
- 18) C. Serre, CERN 67-5 (1967), and private communication.
- 19) L.C.L. Yuan, High-energy physics research (U.S. Government Printing Office, Washington, DC, 1965), p. 449.  
E.M. Purcell, *ibid.* p. 501.

- 20) L.V. Spencer and U. Fano, Phys. Rev. 93, 1172 (1954).
- 21) L.C.L. Yuan, Z. Dimčovski, H. Uto and G.F. Dell, Proposal submitted to the 1972 Tirrenia meeting.

Figure captions

- Fig. 1 : Most probable energy loss for 1 cm A (NTP) versus  $\gamma$  without (dotted curve) and with (solid curve) Sternheimer's<sup>17)</sup> correction for the density effect.
- Fig. 2 : Landau-Vavilov distributions for 100 GeV protons and pions in 1 cm A (NTP).
- Fig. 3 : Pulses obtained in a MWPC: negative on sensitive wires (due to electron collection); positive electrodynamic image (of the sensitive wire pulses) on the HV electrode (proportional to the energy loss of the particle).
- Fig. 4 : Experimental data<sup>9)</sup> (histogram) of energy losses suffered by 374 MeV/c pions in a 1 cm 95% A, 5% C<sub>3</sub>H<sub>8</sub> (NTP). Comparison is made with Landau-Vavilov<sup>1,2)</sup> (corrected by 20% for the finite energy resolution of the counter) and Blunck's distribution<sup>3)</sup> (without correction). The fitted curve shown is used for the Monte Carlo simulations.
- Fig. 5 : Energy losses in argon (NTP) from Sternheimer's<sup>17,18)</sup> theory. If a heavy mass unknown particle losses were to be estimated, the translation properties of the curves should be noticed (the minimum ionizing loss occurs typically at  $p \sim 3 \times$  particle rest-mass).
- Fig. 6 : Maximum likelihood spectra for two kinds of particles A and B differing initially by 5% energy loss difference after 200-layer sampling (layer width  $\sim 1$  cm).
- Fig. 7 : Maximum likelihood spectra for two kinds of particles A and B differing initially by 5% energy loss difference after 400-layer sampling (layer width  $\sim 1$  cm).
- Fig. 8 : Maximum likelihood spectra for two kinds of particles A and B differing initially by 5% energy loss difference after 600-layer sampling (layer width  $\sim 1$  cm).

- Fig. 9 : Maximum likelihood spectra for two kinds of particles A and B differing initially by 10% energy loss difference after 200-layer sampling (layer width  $\sim 1$  cm).
- Fig. 10 : Maximum likelihood spectra for two kinds of particles A and B differing initially by 10% energy loss difference after 400-layer sampling (layer width  $\sim 1$  cm).
- Fig. 11 : Maximum likelihood spectra for two kinds of particles A and B differing initially by 15% energy loss difference after 200-layer sampling (layer width  $\sim 1$  cm).
- Fig. 12 : Maximum likelihood spectra for two kinds of particles A and B differing initially by 15% energy loss difference after 400-layer sampling (layer width  $\sim 1$  cm).
- Fig. 13 : Maximum likelihood spectra for two kinds of particles A and B differing initially by 10% energy loss difference after 200-layer sampling (layer width  $\sim 1$  cm). The fitted curve for the B population was taken with FWHM 20% larger than that of A.
- Fig. 14 : Schematic set-up of the multilayer detector.

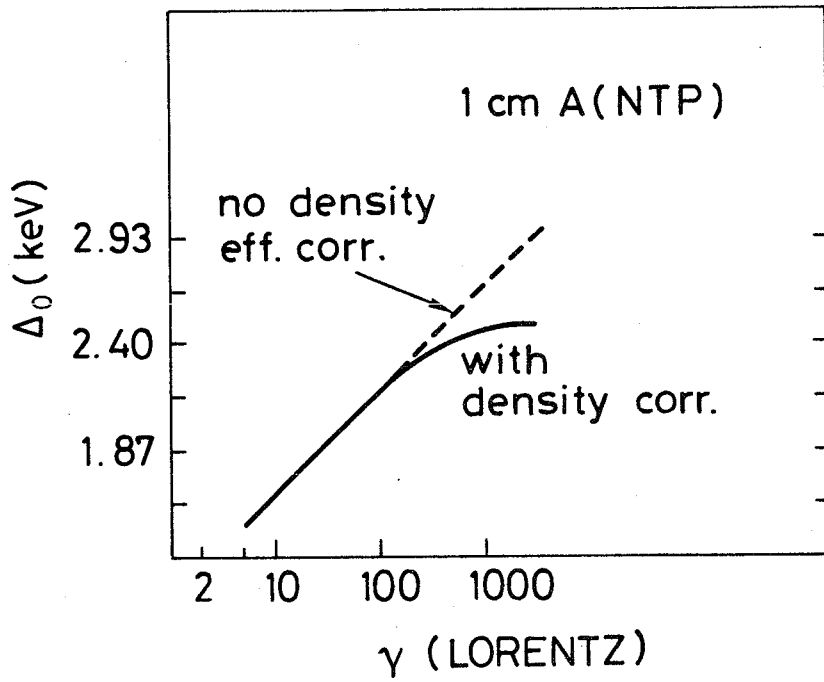


Fig. 1

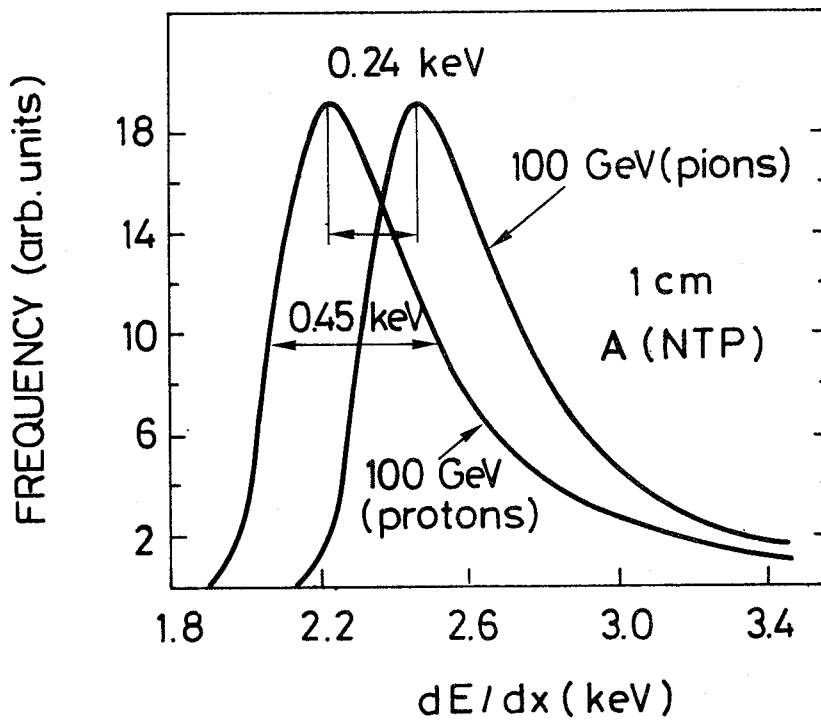


Fig. 2

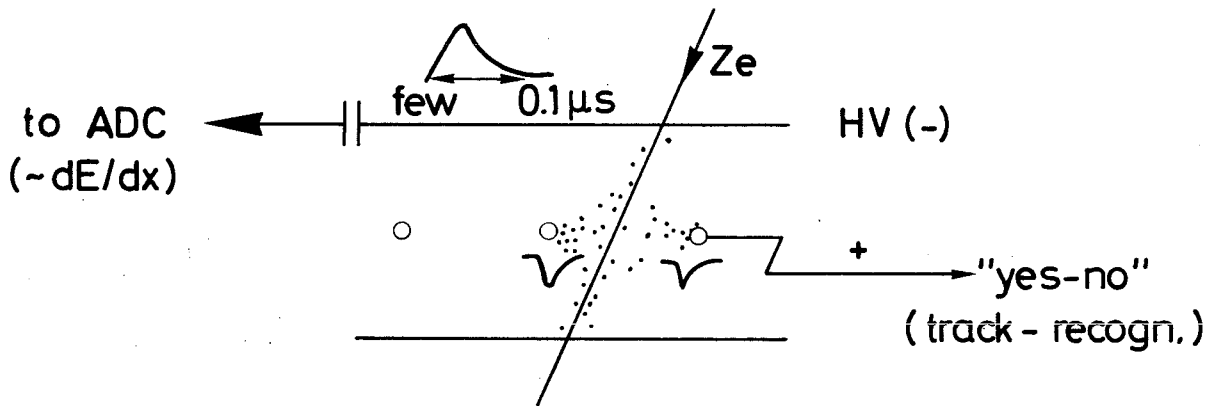


Fig. 3

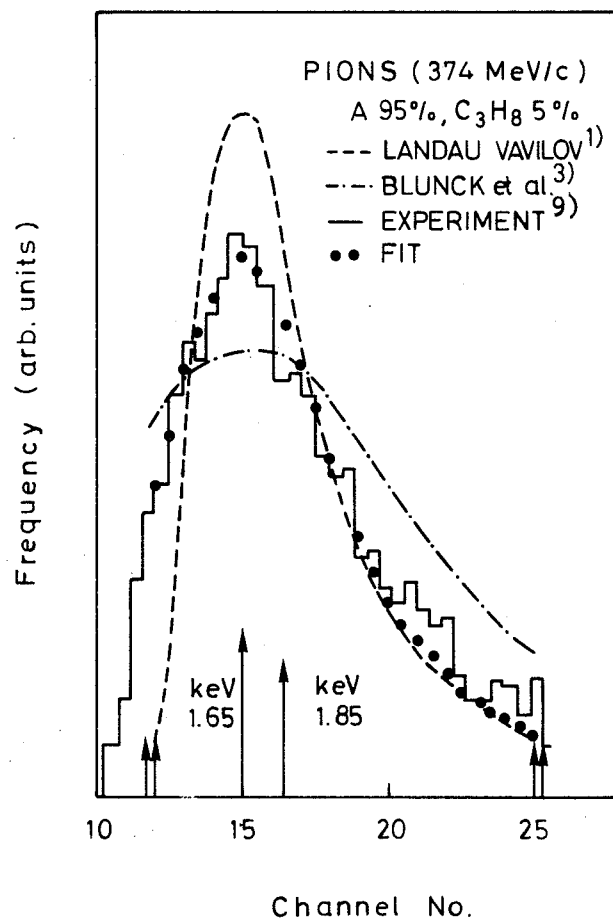


Fig. 4



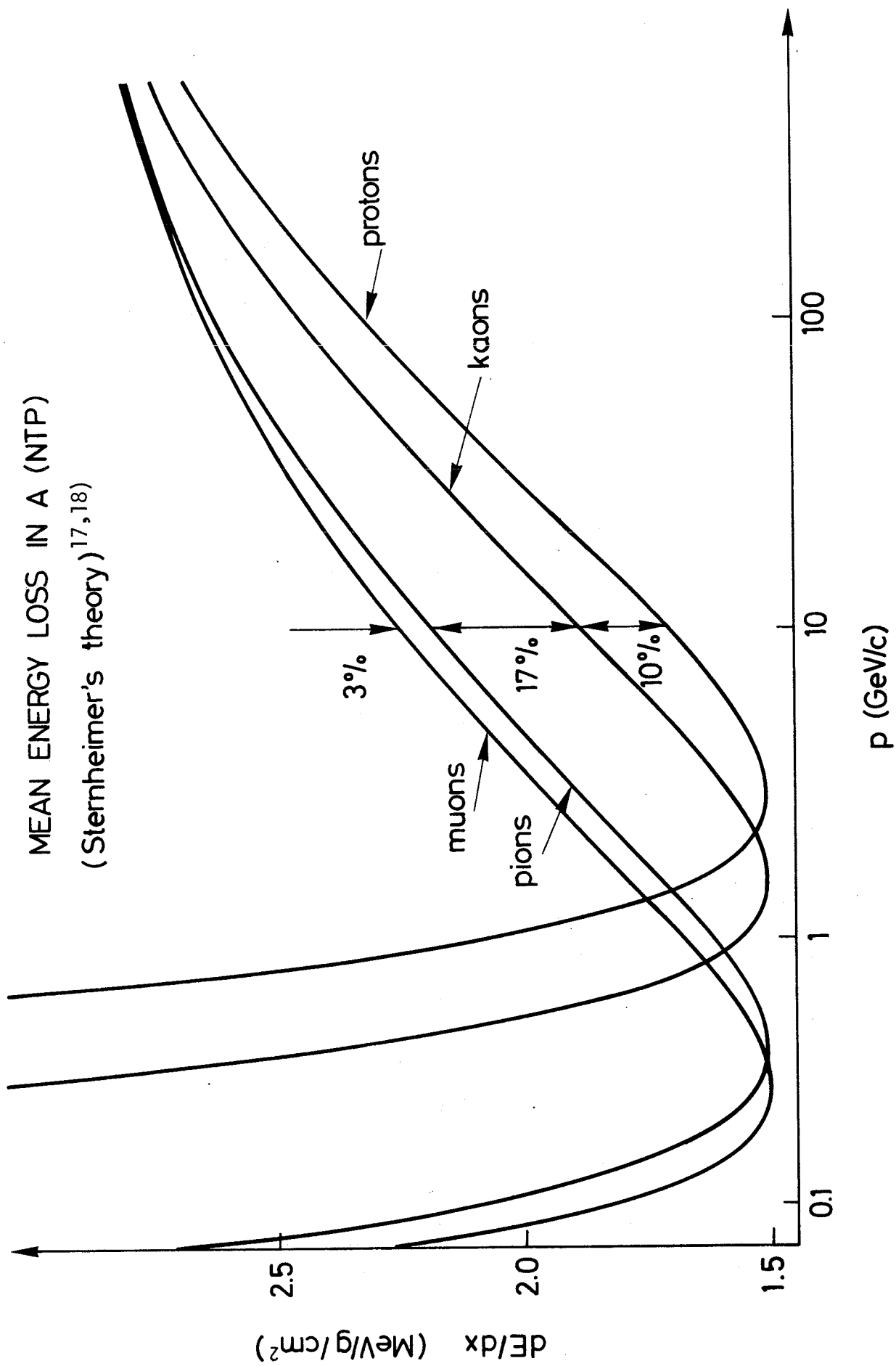


Fig. 5

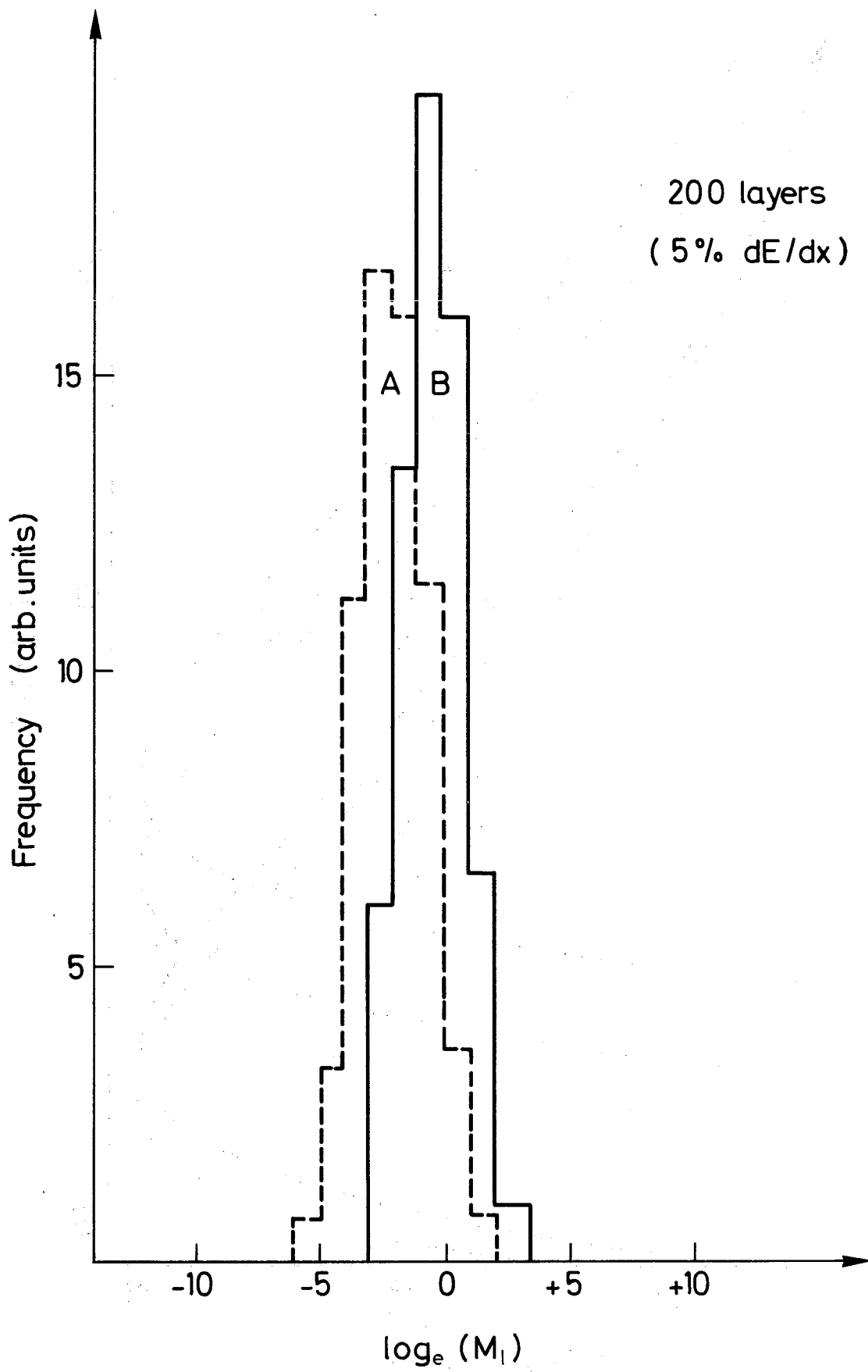


Fig. 6

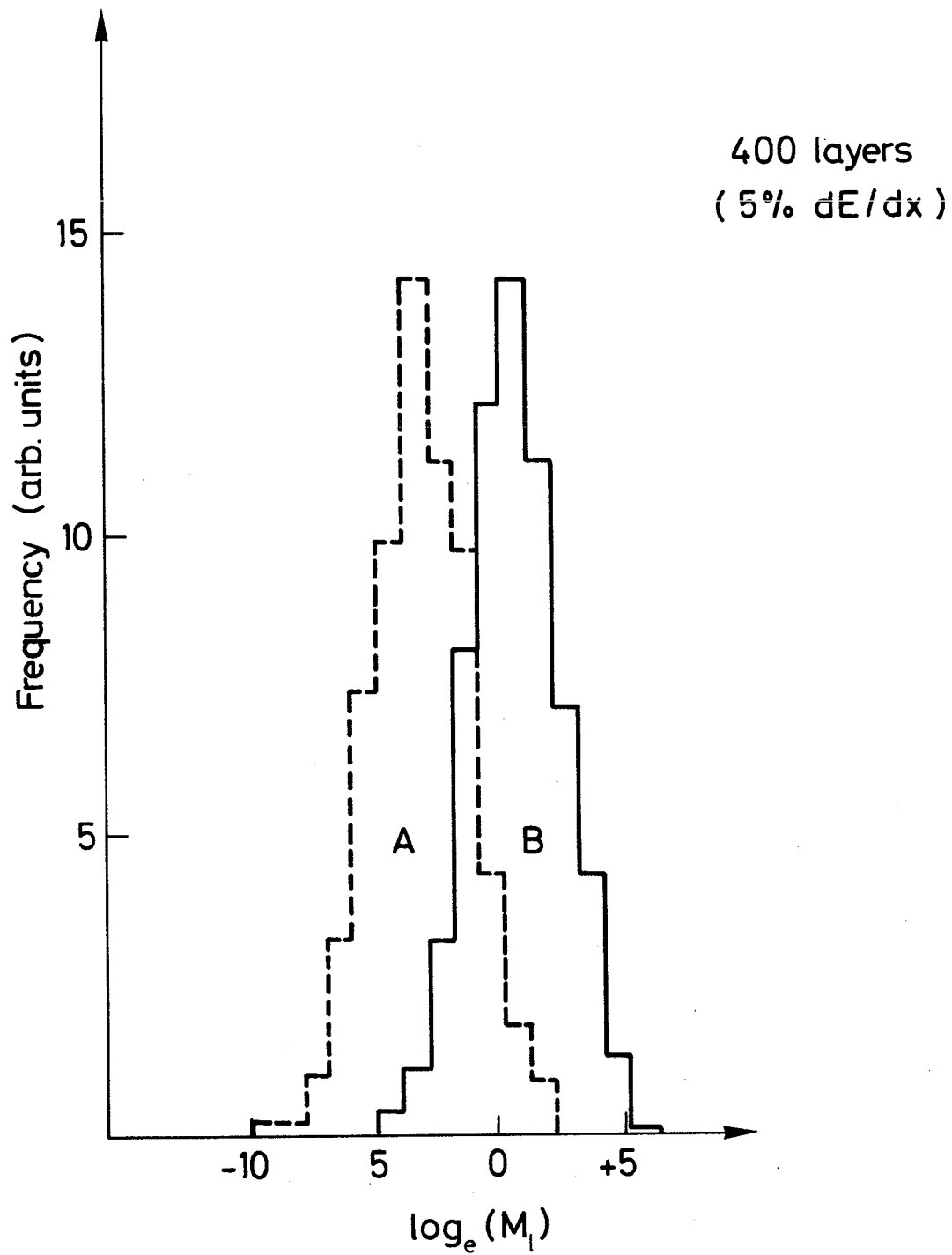


Fig. 7

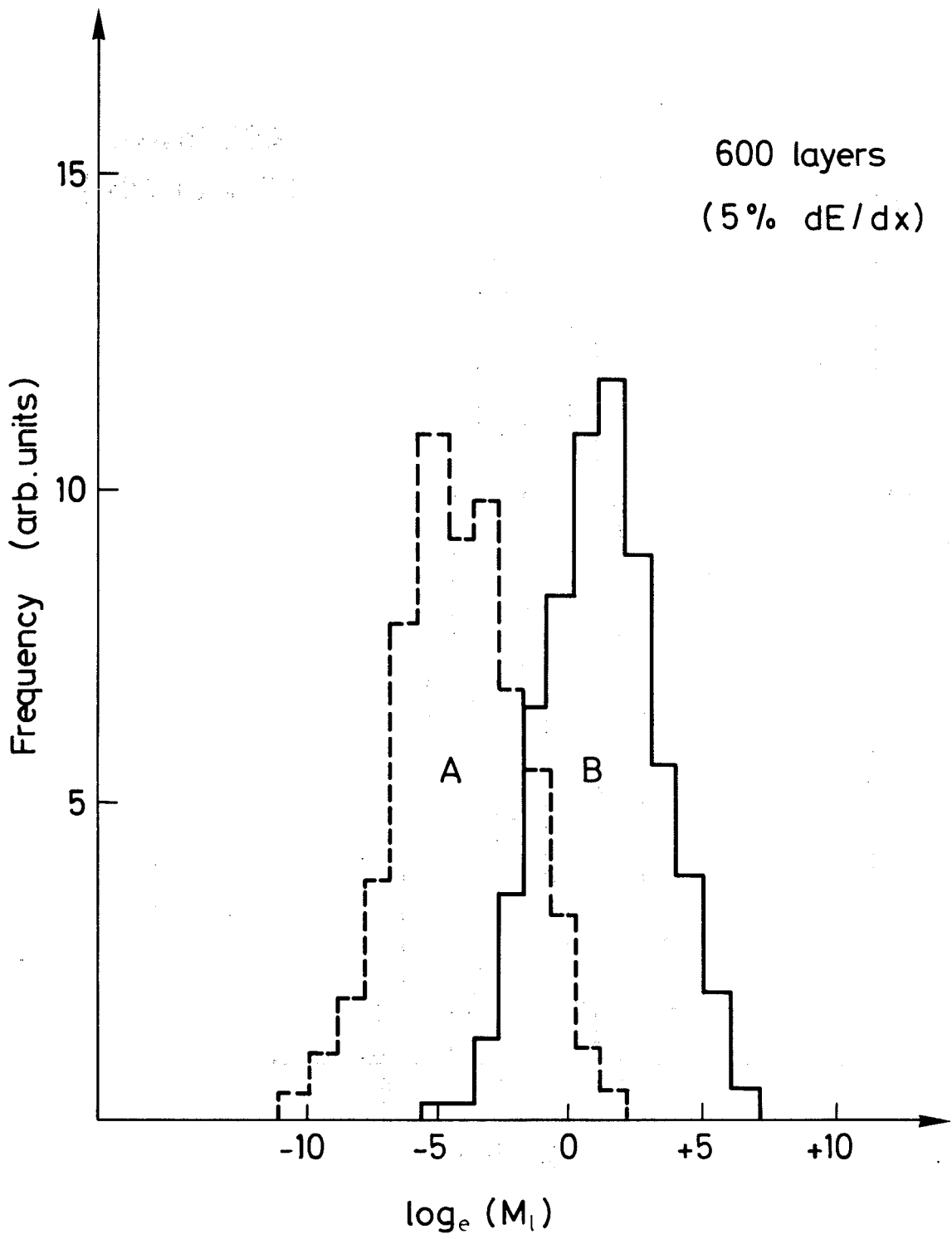


Fig. 8

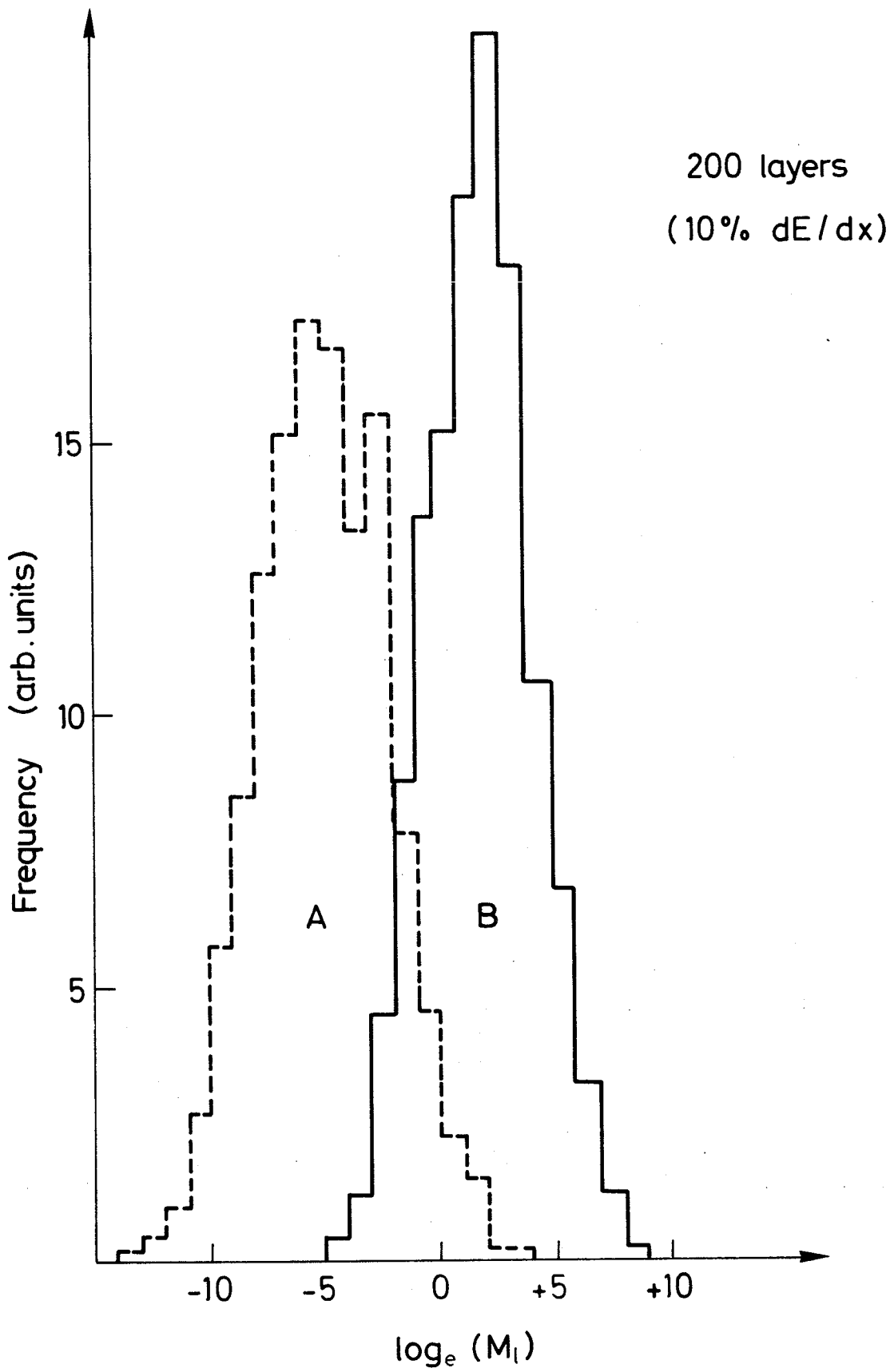


Fig. 9

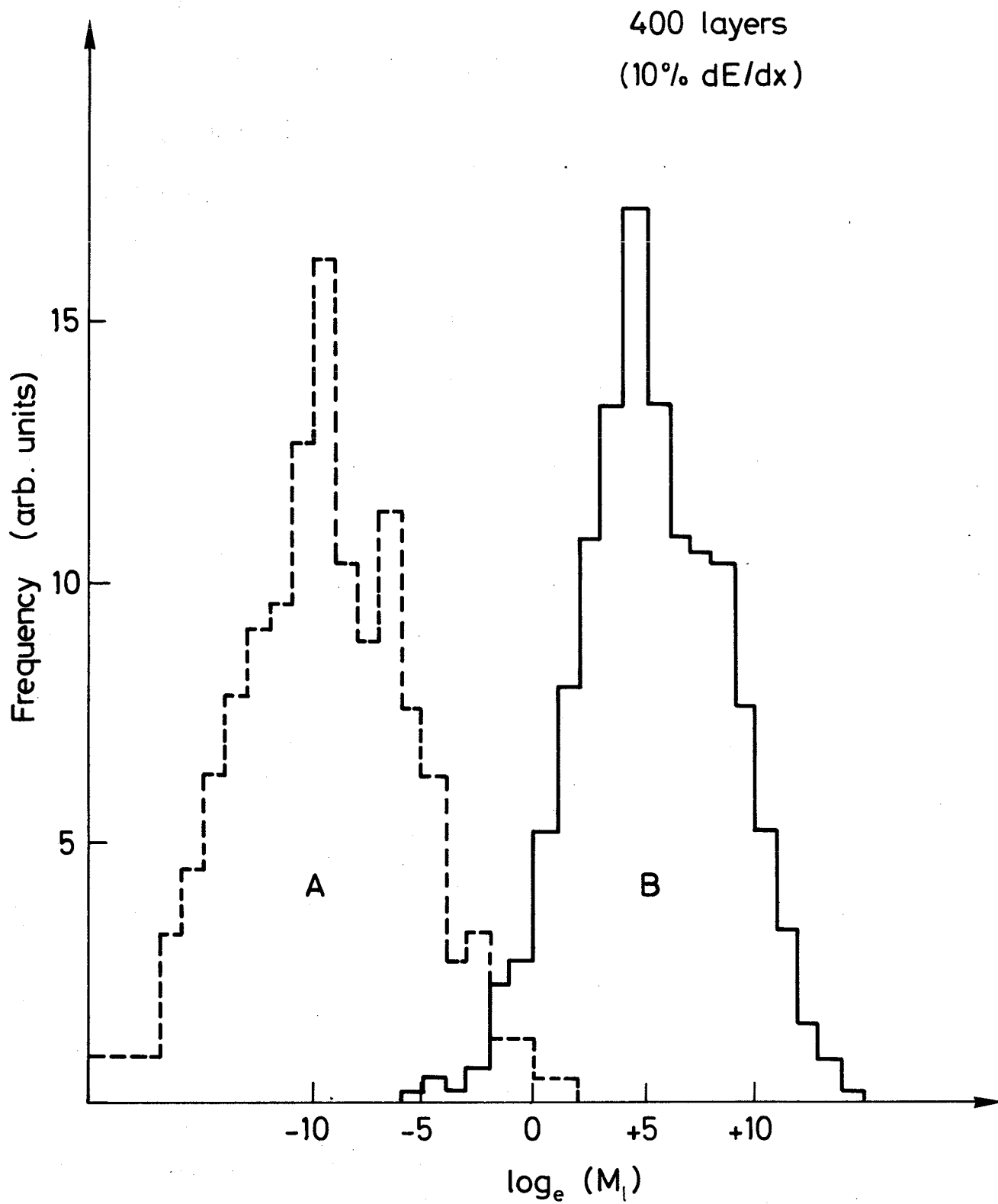


Fig. 10

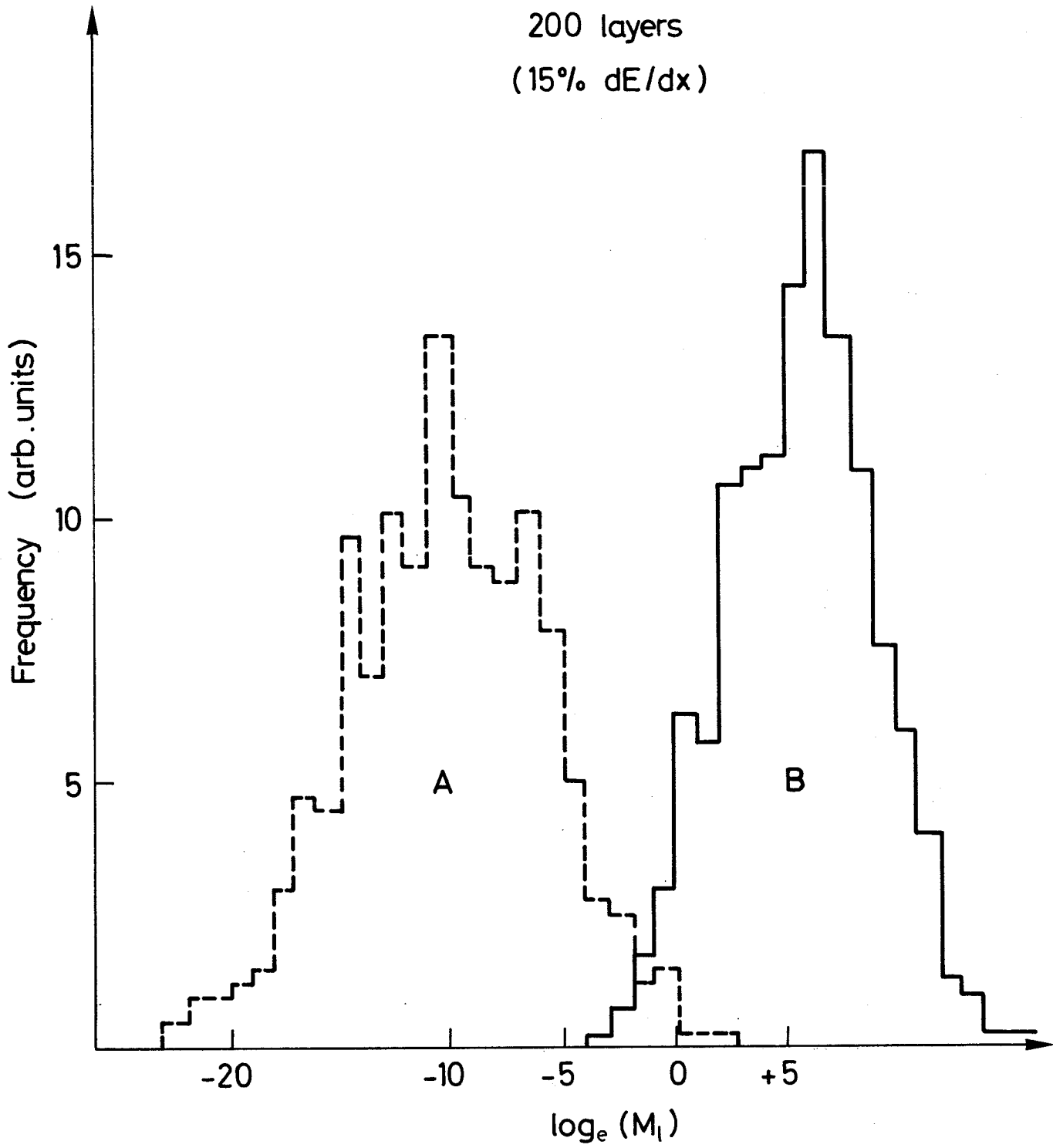


Fig. 11

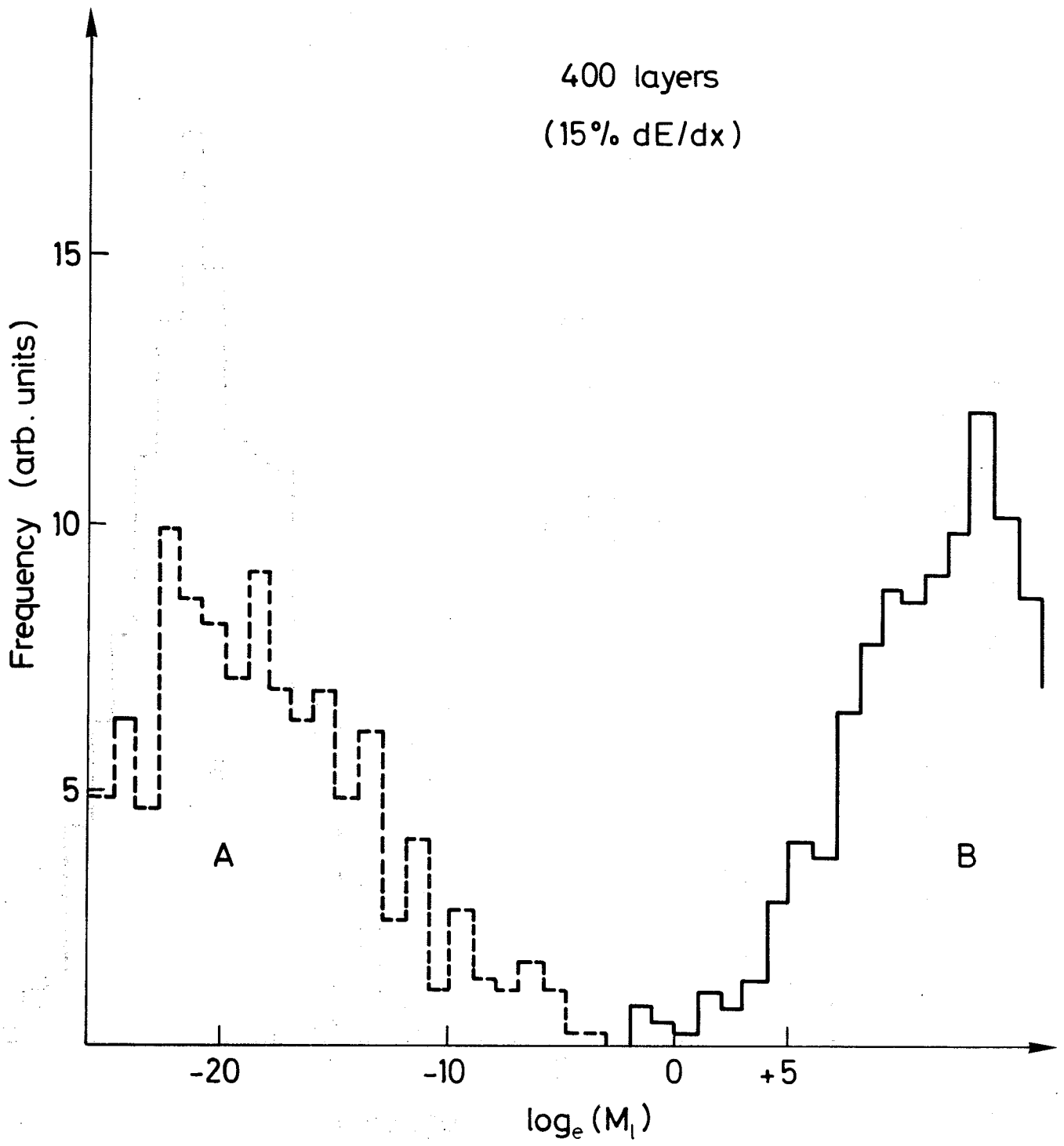


Fig. 12



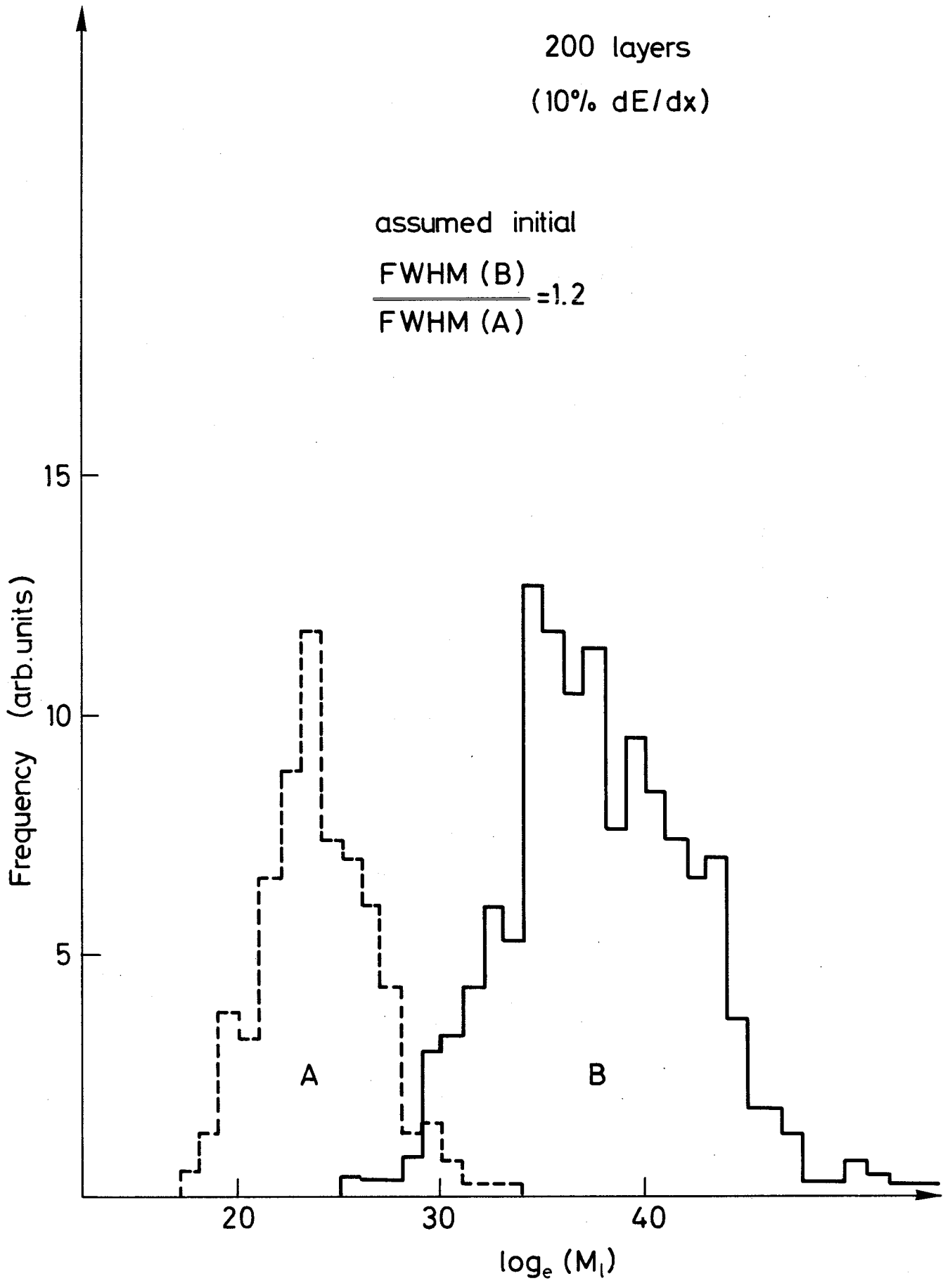


Fig. 13

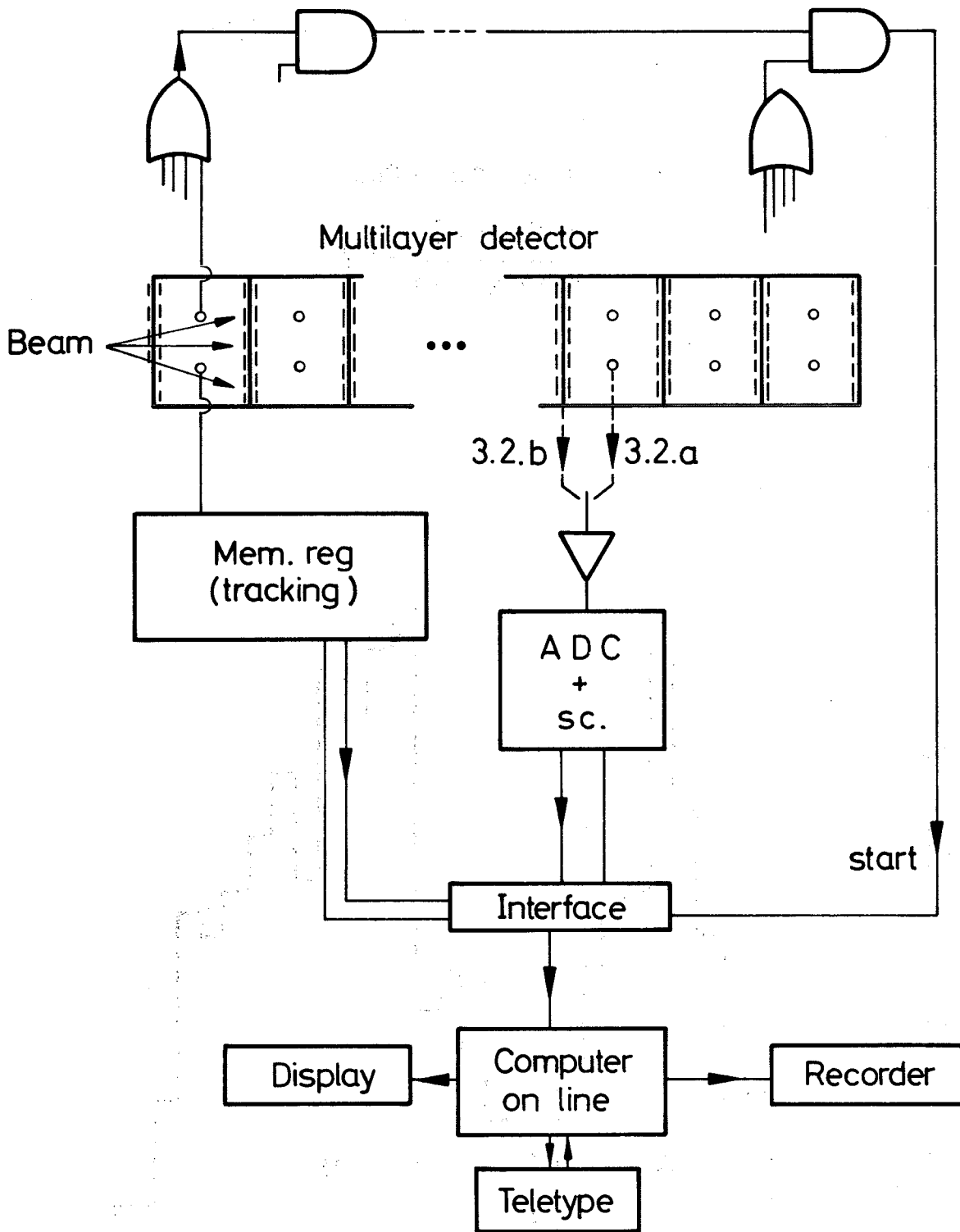


Fig. 14

